Studying High Energy EGRET Sources by an Array of Water Cherenkov Detectors

By Shima Bayesteh

Aloborz Observatory
Sharif University of Technology

What are components of cosmic rays?

Almost 90% of all the incoming cosmic ray particles are simple protons, with nearly 10% being helium nuclei (alpha particles), and slightly under 1% are heavier elements, electrons (beta particles), or gamma ray photons.

Upto 50s before the first particle accelerators were built, studying cosmic rays was a useful way of discovering new particles .

1932 — Karl Anderson discovered a new charged particle from its trace in Cloud chamber, called Positron.

1937 — Anderson and Neddermeyer detected Muon as a component of secondary cosmic ray particles.

1940 — Bruno Rossi in 1934 and Auger in 1937, observed **Air shower** of secondary cosmic ray particles.

What is Air Shower?

Developement of Cosmic Ray Air Shower

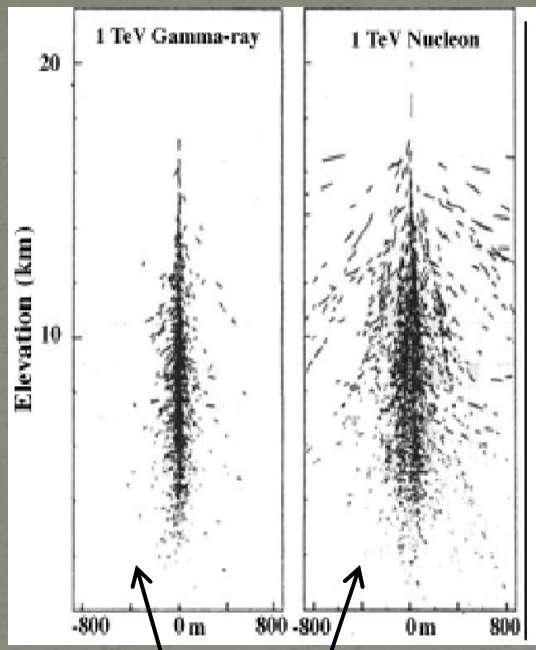

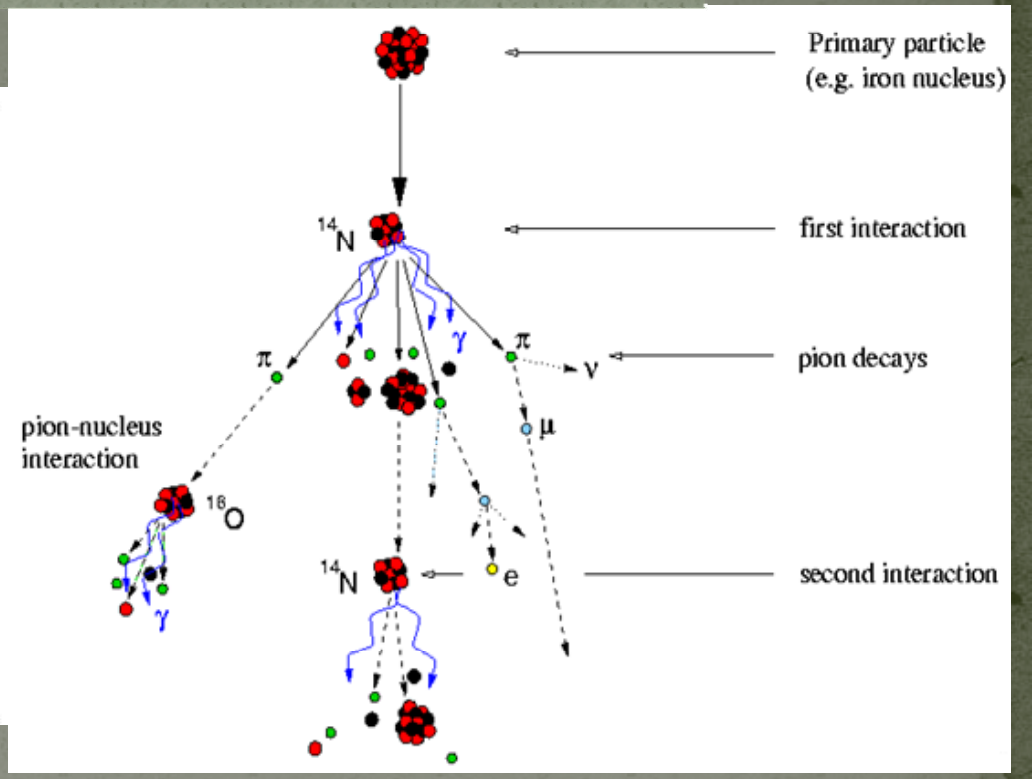

- **Hadronic Air Showers:** Originate from primary charged particles most probable Protons or nuclei of an atom.
- **Electromagnetic Air Showers:** Initiate from a primary high energy gamma ray photons pointing gamma ray sources in the sky.

The following Fig shows change in cosmic rays flux for a wide range of energy. The graph is logarithmic .

$$\frac{dN}{dE}\left(m^{-2}sr^{-1}s^{-1}GeV^{-1}\right) \approx 1.8E^{-\gamma}$$

Up to E~10^6 GeV, γ=2.7 and more than this γ=3.

Based on interactions predicted between the cosmic rays and the photons of the CMB radiation, GZK limit was computed by Greisen and Kuzmin and Zatsepin cosmic rays with energies over 6×10^{19} eV would interact with cosmic microwave background photons to produce Pions.

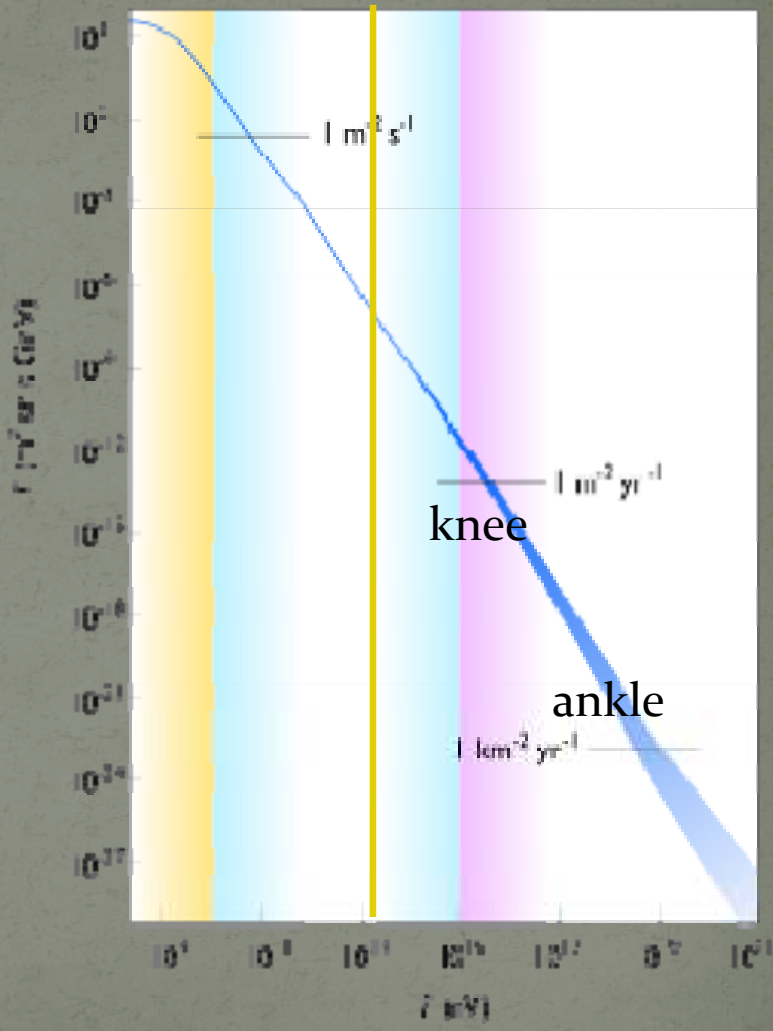

Gamma Ray Detection

- Detecting gamma ray photons with higher flux and lower energy by satellites and ballons.

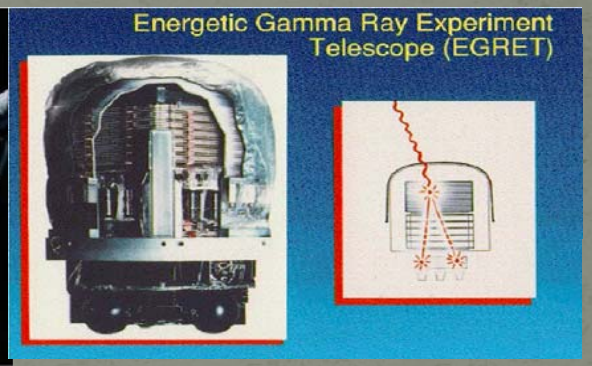

- Very energetic gamma-rays can also be detected by ground based experiments. The Imaging Atmospheric Cherenkov Telescope technique currently achieves the highest sensitivity.

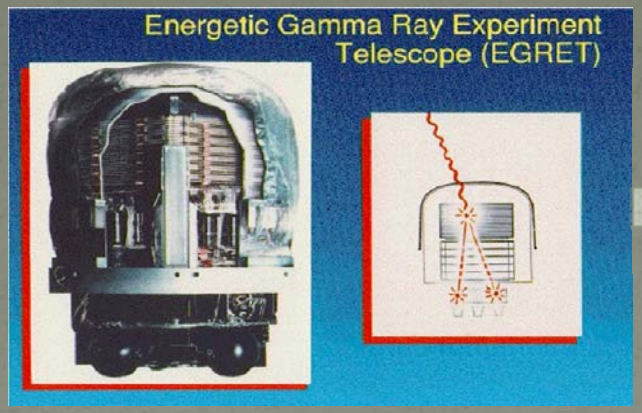

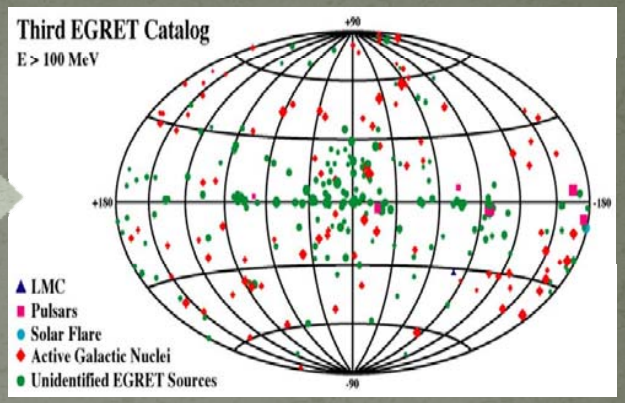

100MeV >E <30GeV

E>10TeV ?

If there is any source in EGRET which emits higher energetic photons to produce Electromagnetic EASs, detectable by our ground-based array with energy threshold of>10TeV.

Applied Water Chrenkov Detectors in ALBORZ Observatory

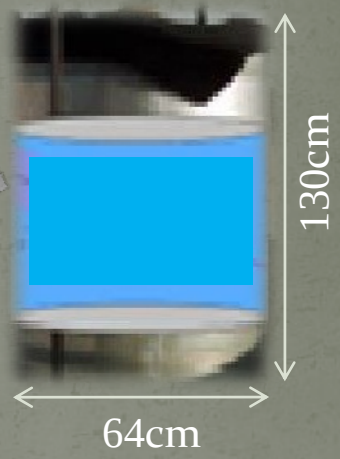

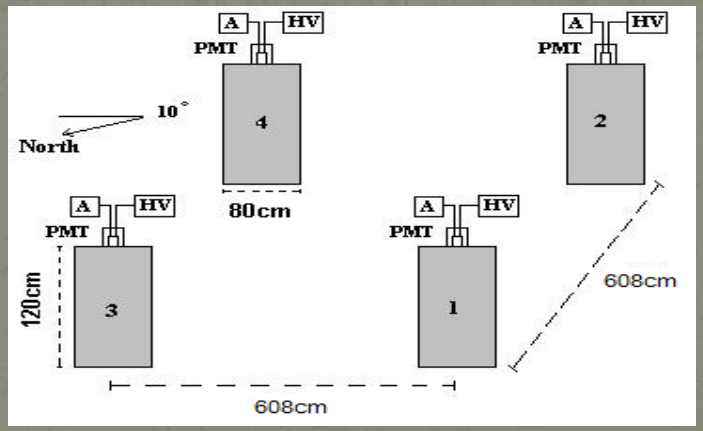

Electronic circuit of the WCD array

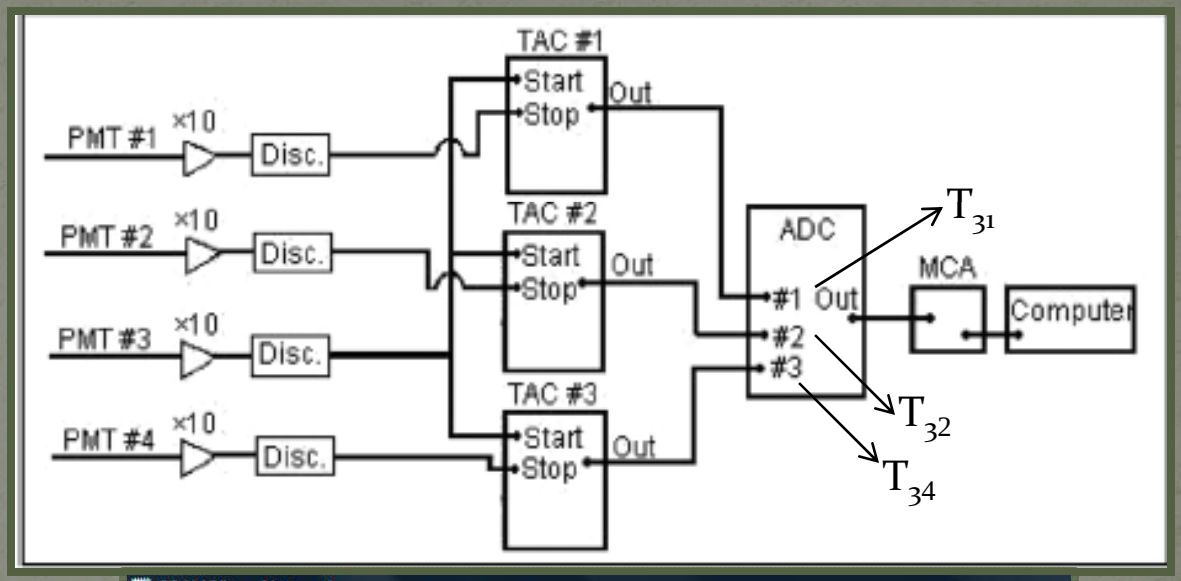

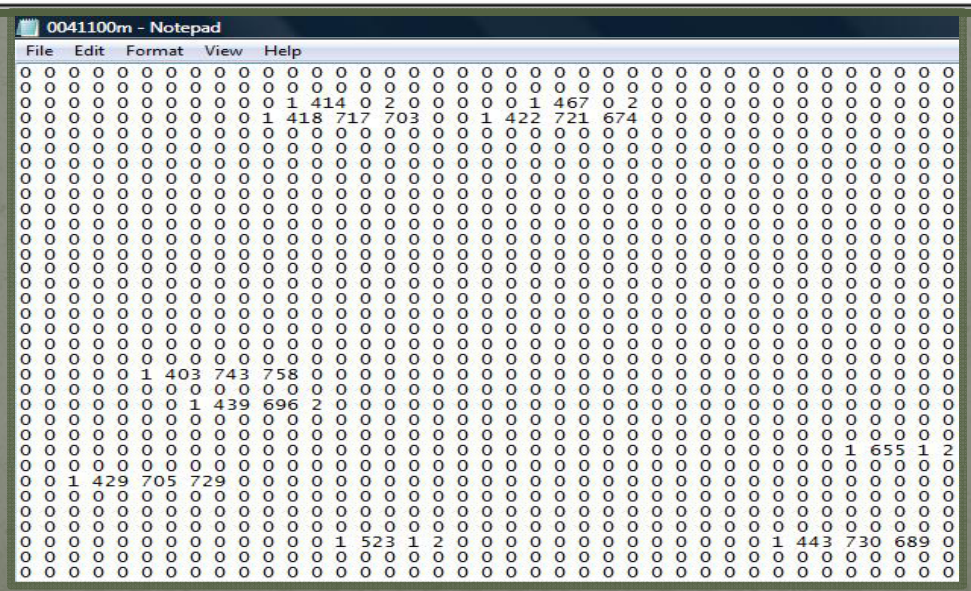

Finding arrival angle of EAS events

$$X = c\begin{vmatrix} \sum \alpha_i T_{3i} & \sum \alpha_i \beta_i \\ \sum \beta_i T_{4i} & \sum \beta_i^2 \end{vmatrix} \Big/ \begin{vmatrix} \sum \alpha_i^2 & \sum \alpha_i \beta_i \\ \sum \alpha_i \beta_i & \sum \beta_i^2 \end{vmatrix} \qquad Y = c\begin{vmatrix} \sum \beta_i T_{3i} & \sum \alpha_i \beta_i \\ \sum \alpha_i T_{4i} & \sum \alpha_i^2 \end{vmatrix} \Big/ \begin{vmatrix} \sum \alpha_i^2 & \sum \alpha_i \beta_i \\ \sum \alpha_i \beta_i & \sum \beta_i^2 \end{vmatrix}$$

$$\theta = \tan^{-1}\sqrt{\frac{X^2+Y^2}{1-X^2-Y^2}}, \qquad \varphi = \tan^{-1}\left(\frac{Y}{X}\right)$$

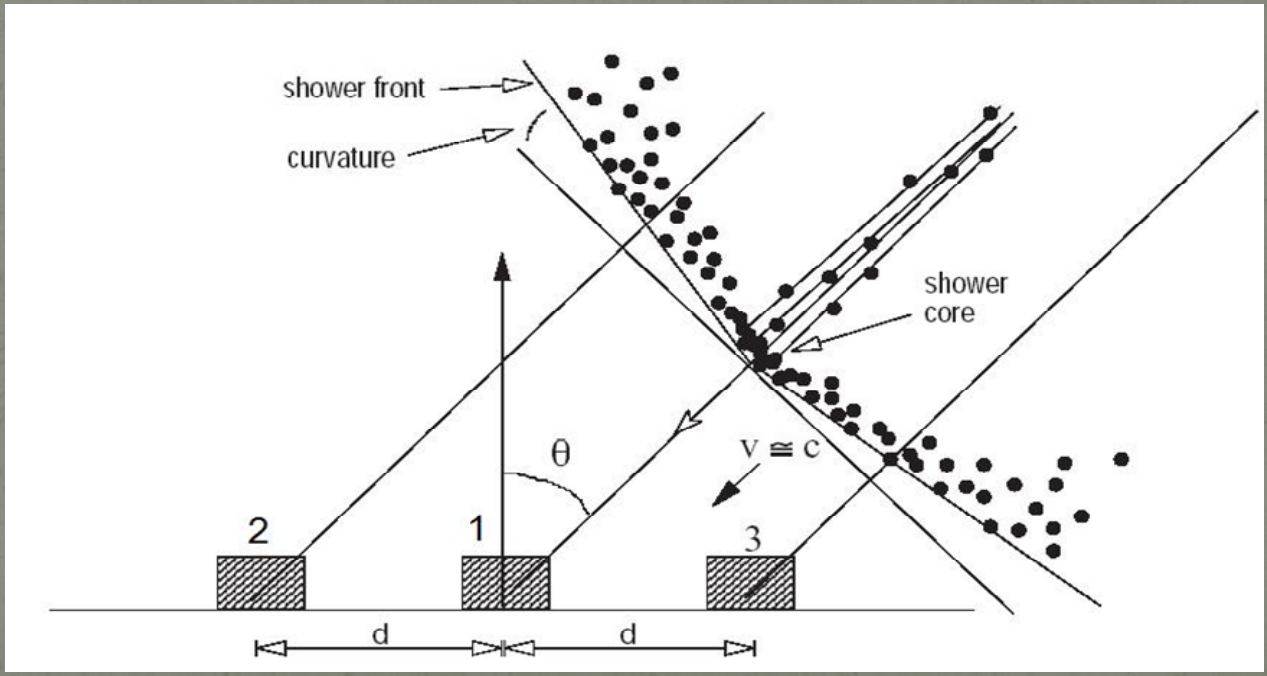

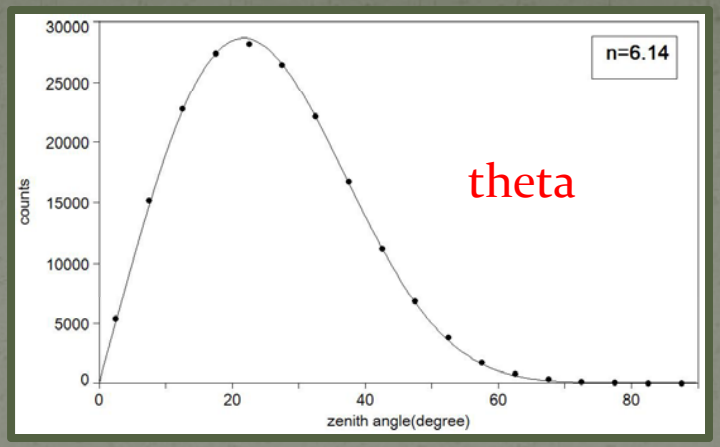

theta

$$\frac{dN}{d\theta} = A_o(B_1 \cos\theta + B_2 \sin\theta)\sin\theta\cos^n\theta$$

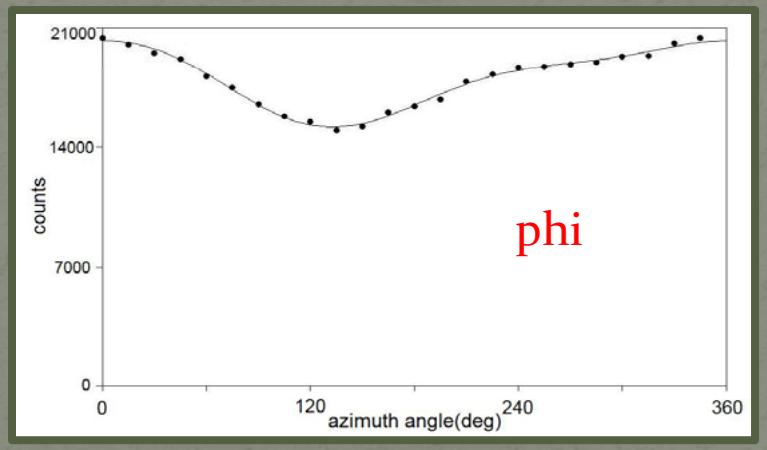

phi

$$\frac{dN}{d\varphi} = A_o[1 + A_1\cos(\varphi - \varphi_1) + A_2\cos(2\varphi - \varphi_2)]$$

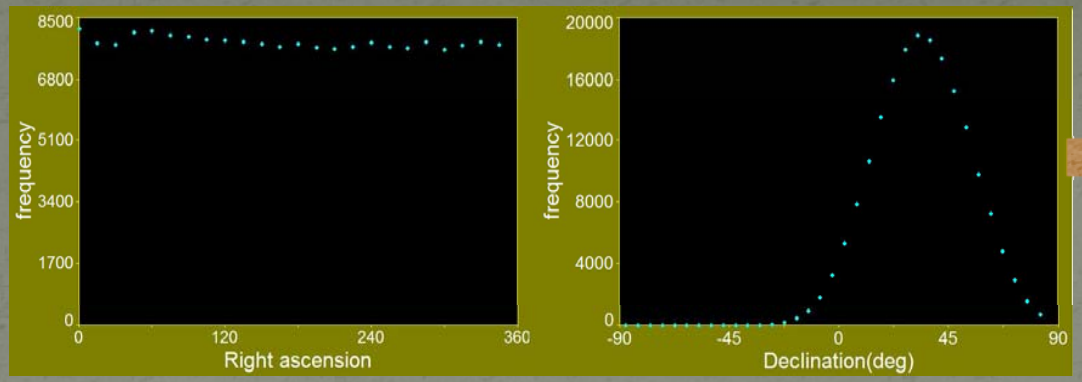

Right ascension and Declination distribution

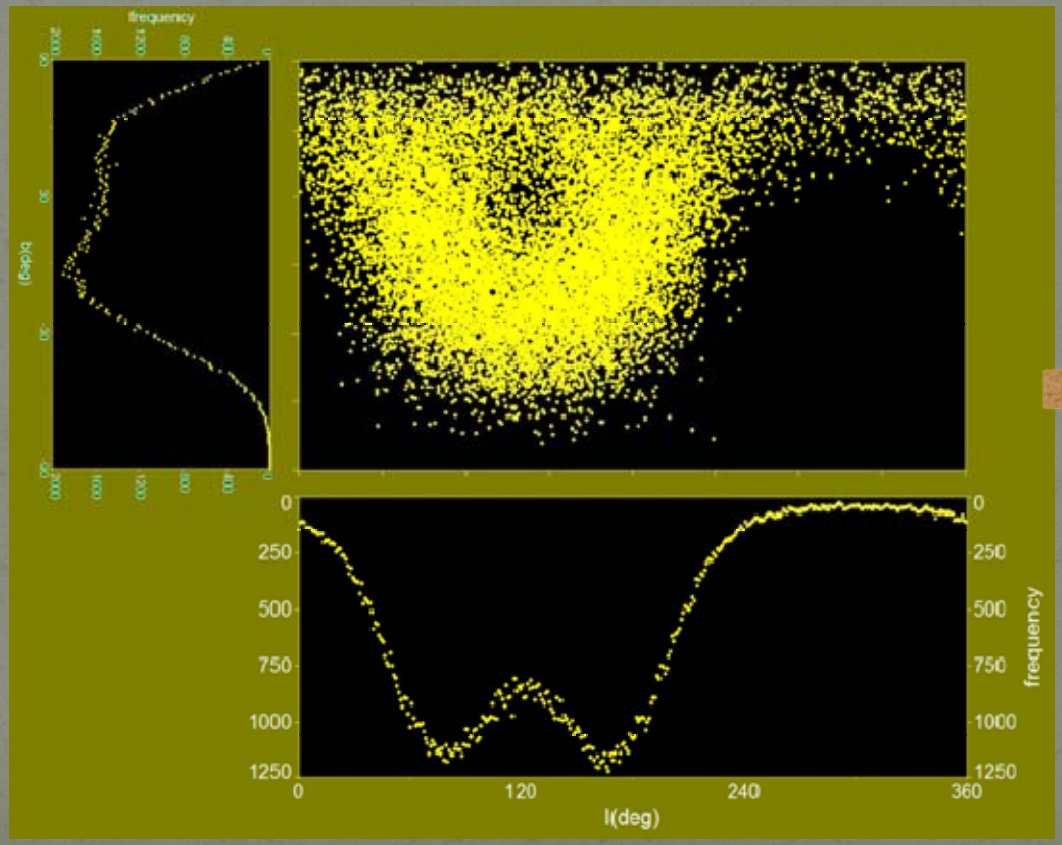

Galactic map with galactic latitude and longitude distribution

- According to alt-azimuth angular distribution and total number of events, 604000, we provided an exposure galactic map.
- we divided the data galactic map by the exposure galactic map pixel by pixel.

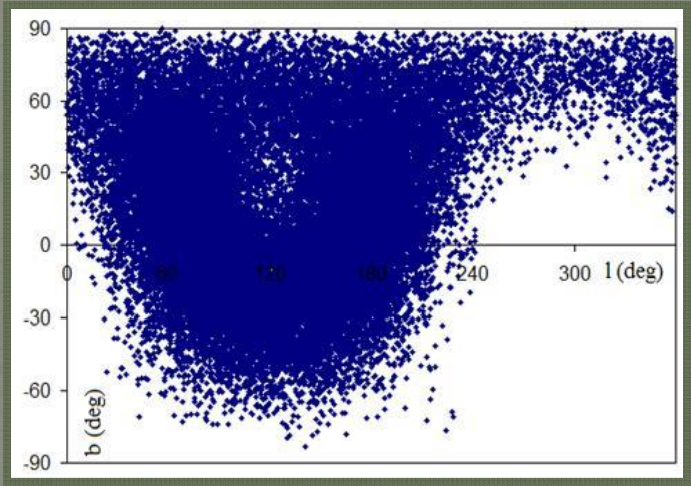

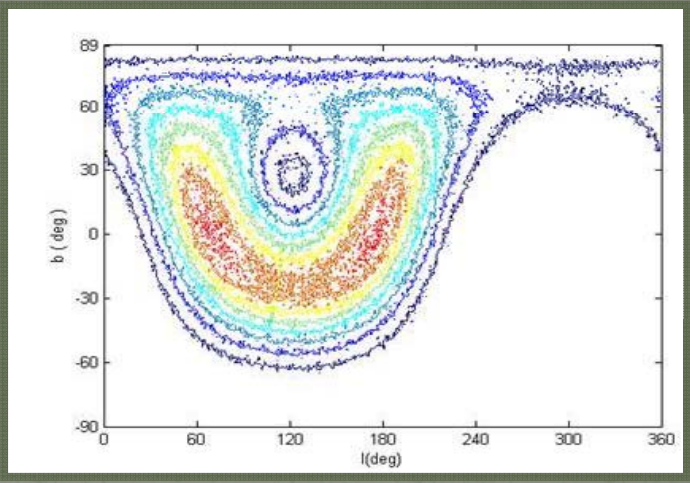

- we looked for excess emission that could be from gamma ray sources. We used the third EGRET catalogue as a reference. Finding important excesses we employed Li-Ma method .

On $\longrightarrow$ $\sqrt{2}r_e$

n_s =full pixels in this region.
N_{on} = counts in this region

off $\longrightarrow$ $2r_e$

n_b =full pixels in this region
N_{off} = counts in this region

$\Delta\Omega = \cos b\, \Delta b\, \Delta l$

$r_e \cong (\Delta\Omega/\pi)^{1/2}$

$$S = \frac{N_{on} - \alpha N_{off}}{\sqrt{N_{on} + \alpha^2 N_{off}}}$$

$$\alpha = \frac{n_s}{n_b}$$

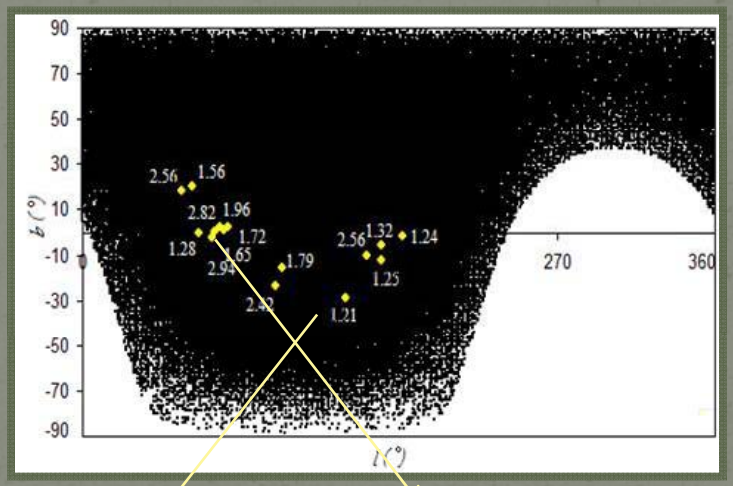

3EG J0240+2816 3EG J2033+3716

name	ID	L_d	b_d	σ_{cher}	σ_{scin}	r_e
3EG J0239+2816	a	150.21	-28.8	1.215	1.606	6.58
3EG J0416+3650	a	162.22	-9.97	2.558	-0.682	6.93
3EG J0433+2908	A	170.48	-12.58	1.245	0.097	6.93
3EG J0459+3352		170.3	-5.38	1.319	-0.226	6.99
3EG J0542+2610		182.02	-1.99	1.245	-0.288	6.99
3EG J1824+3441		62.49	20.14	1.56	-1.436	6.81
3EG J1825+2854		56.79	18.03	2.562	0.225	6.81
3EG J1958+2909		66.23	-0.16	1.284	-1.293	6.99
3EG J2020+4017		78.05	2.08	1.962	0.479	6.99
3EG J2021+3716		75.58	0.33	2.822	1.079	6.99
3EG J2027+3429		74.08	-2.36	2.949	0.225	6.99
3EG J2033+4118		80.27	0.73	1.657	-0.970	6.99
3EG J2035+4441		83.17	2.5	1.724	0.068	6.99
3EG J2352+3752	a	110.26	-23.54	2.423	-0.802	6.70
3EG J2358+4604	A	113.39	-15.82	1.79	0.590	6.87

We obtain count in subinterval distributions for any time interval. As we expect, the majority of recorded extensive air showers arrive randomly to our array and if we acquire count in time intervals distributions, they are Poissonian. The poisson distribution is a Discrete probability distribution that expresses the probability of number of events occurring in a fixed period of time ,if these events occur with a known mean rate and independently of the time since the last event.

$$P(x) = N_o \frac{e^{-\lambda}\lambda^x}{x!}$$

We separate this time period into time intervals in two ways, and for each period we consider subintervals or time windows: 10, 30, 100, 300, 1000 and 3000 seconds.

1. Separating one year into 6 two-months.
2. according to change in count rate up to just 10 percent we will have new divisions, three parts that with a good accuracy we can say that count rate in these parts is stable. Durations of new parts are not equal

Two month is long enogh to have adequate data to analyze, on the other hand in this time interval count rate stays steady.

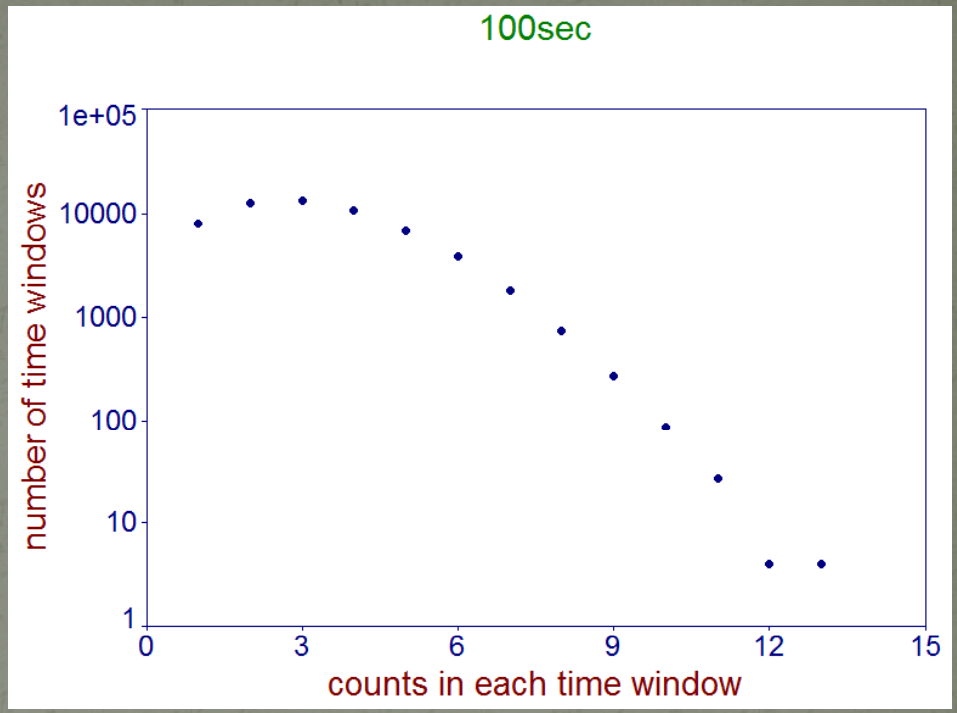

2months

Subintervals:
10sec, 30sec, 100sec ,
300sec, 1000sec, 3000sec

Counts in each time-window distribution for the first two-month.

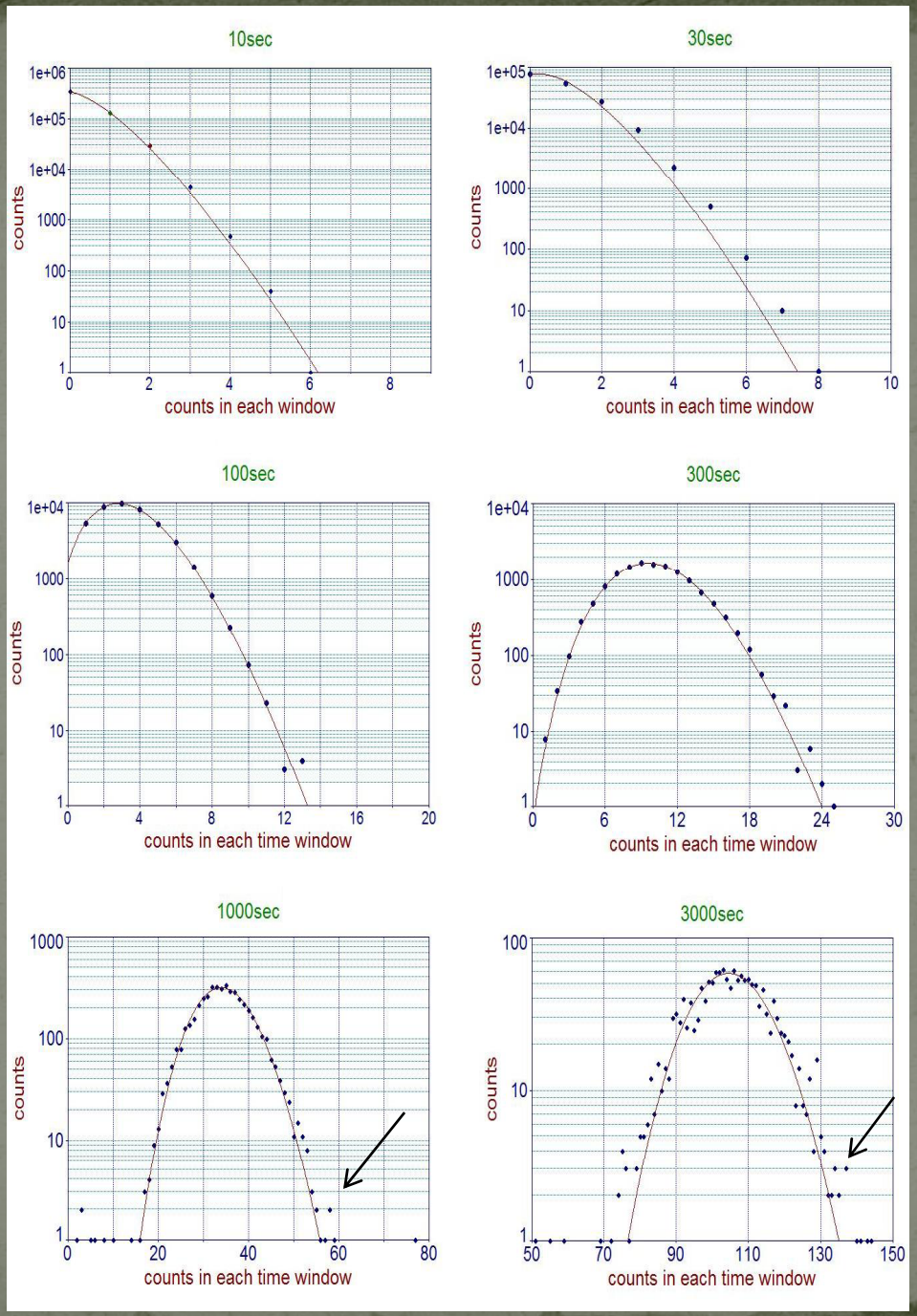

Results and simlar events and their related time windows obtained from the first separation.

	1st -2month	2nd -2month	3rd -2month	4th -2month	5th -2month	6th -2month
Mean count rate	0.00673	0.00617	0.00544	0.00405	0.00385	0.00351
Similar events in two time windows	12	12	-------	-------	155	41
Time windows related to raw 2	(30 ,300) (300 ,1000)	(100 ,300)	-------	-------	(30 ,100) (300 ,1000) (1000 ,3000)	(10 ,300) (30 ,1000)
similar events in three time windows	0	0	----------	---------	24	
Time windows related to raw 2	---------	----------	---------	-------	(30 ,100 ,1000) (300 ,1000 ,3000)	--------

24similar events in three time windows
300sec, 1000sec, 3000sec

	L	B	DEC	RA	θ	φ	Time
1	133.5	-46.6	15.6	19.5	28.4	127.0	3:05
2	89.1	-44.6	11.9	348.3	24.1	199.6	3:05
3	86.1	-31.5	21.7	338.8	20.3	234.1	3:05
4	115.1	-42.9	19.5	5.9	17.5	149.0	3:05
5	107.8	1.0	60.1	340.6	27.2	342.6	3:05
6							

	L	B	DEC	RA	θ	φ	time
1	126.4	-7.6	55.1	18.0	26.5	327.2	5:40
2	135.6	-34.5	27.2	23.7	18.2	250.4	5:40
3	170.2	7.6	41.2	87.5	34.9	66.1	5:40
4	175.6	-37.7	8.5	51.5	27.5	161.8	5:40
5	153.7	-10.7	41.8	54.3	11.0	48.5	5:40
6	146.7	-1.8	53.0	54.1	19.6	19.6	5:40
7	140.6	-10.8	48.3	38.7	13.8	347.2	5:40
17	65.9	-33.5	8.7	327.1	38.1	233.9	3:05

In the second step we separate one year into intervals according to stability of mean count rate up to 90% of the maximum count rate, so we have 3 parts.

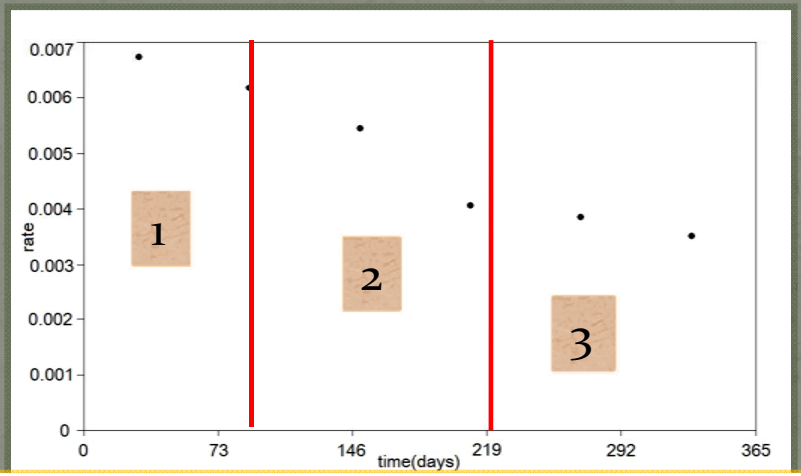

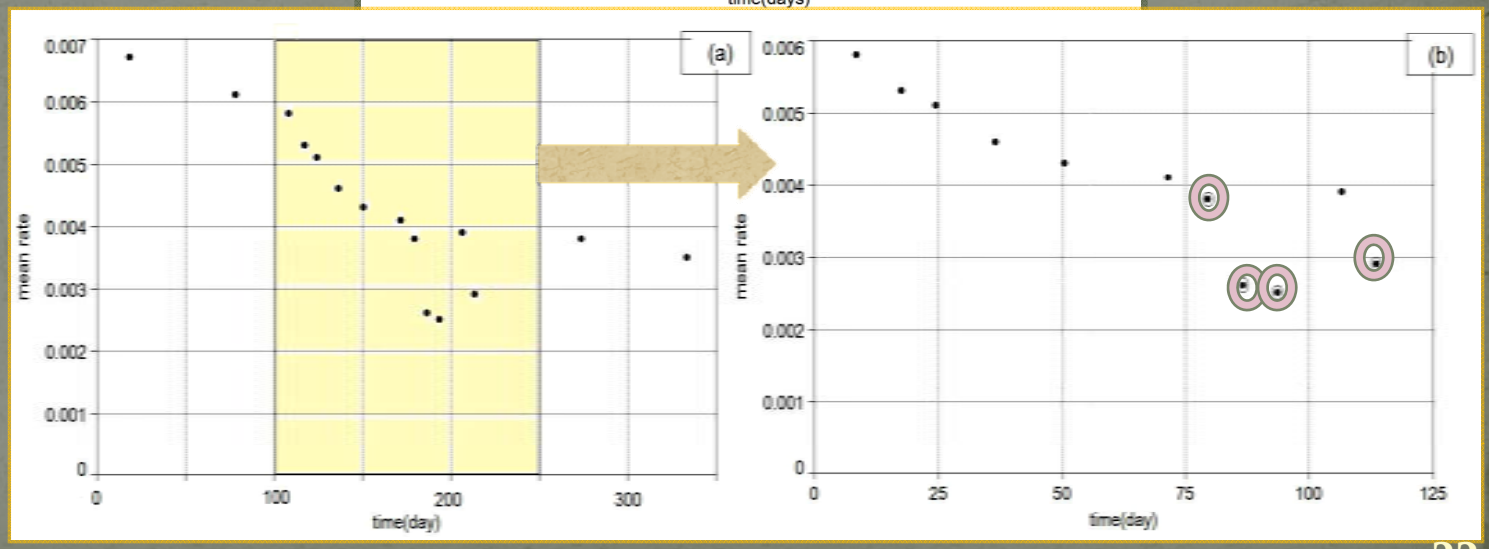

Counts in each time-window distribution for the first part.

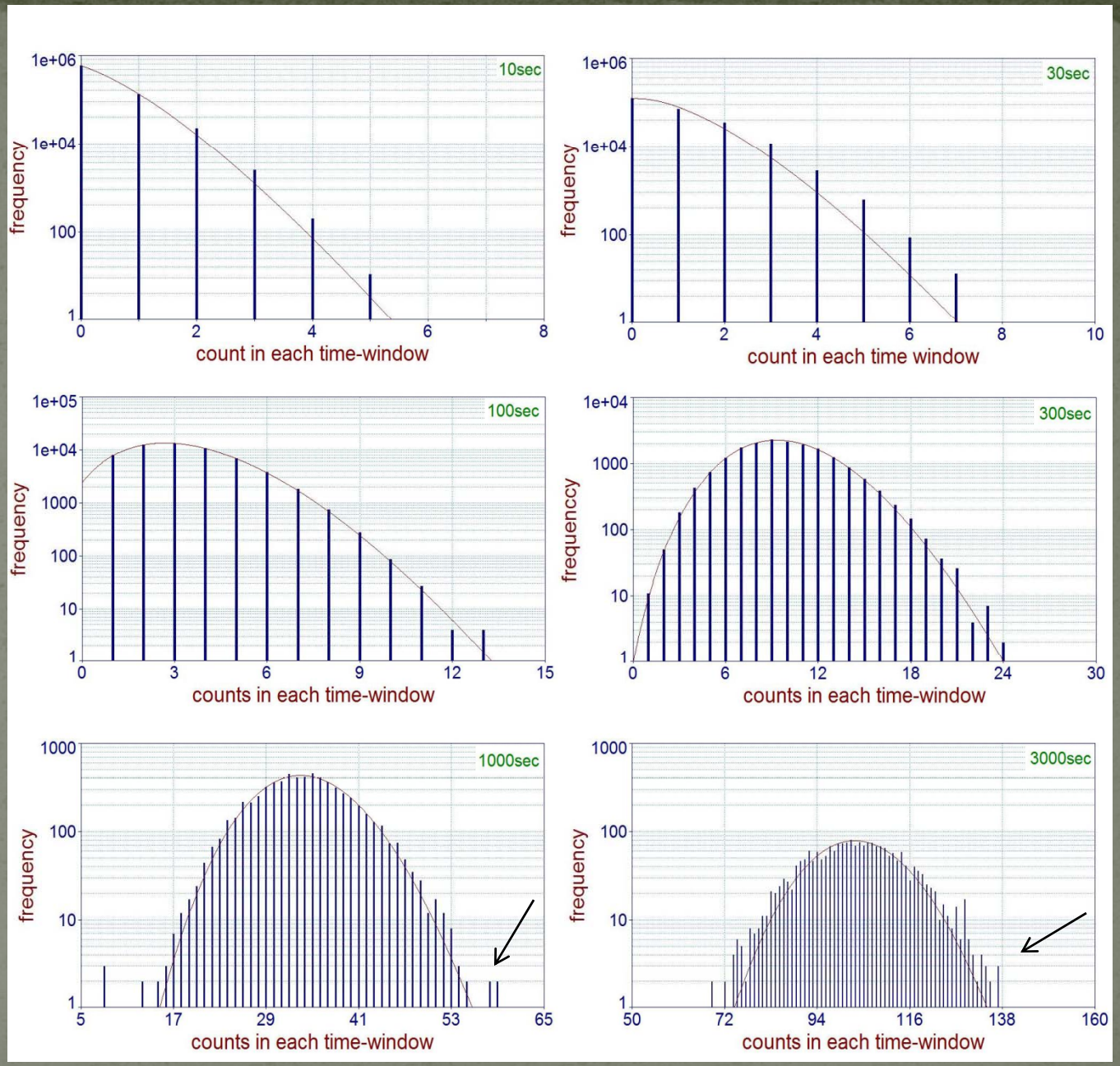

Results and simlar events and their related time windows obtained from the second separation.

	1st part	2nd part	3rd part
Mean count rate	0.00617	0.00570	0.00370
Similar events in two time windows	59	85	84
Time windows related to raw 2	3000 ,1000	3000,1000,300	30,100,300,1000
similar events in three time windows	0	17	7
Time windows related to raw 2	**0**	3000,1000,300	1000,300,100
time interval of each part	06/11/19-07/02/14	07/02/10-07/04/16	07/05/1**9**-07/11/20

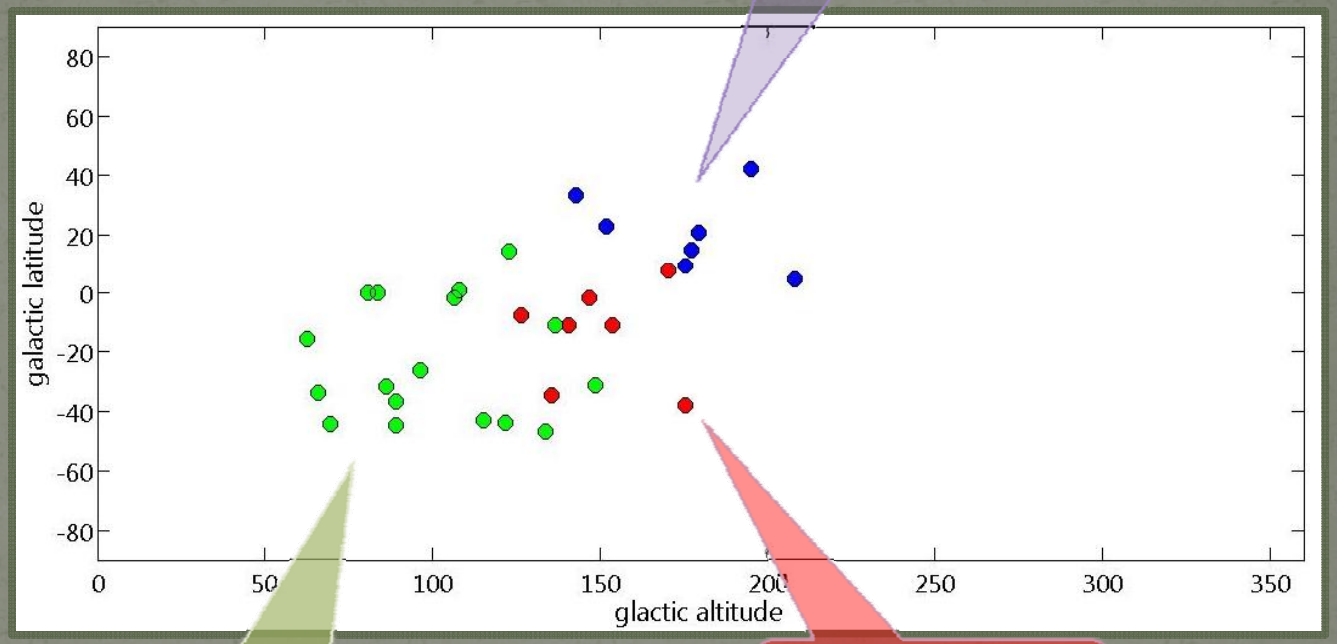

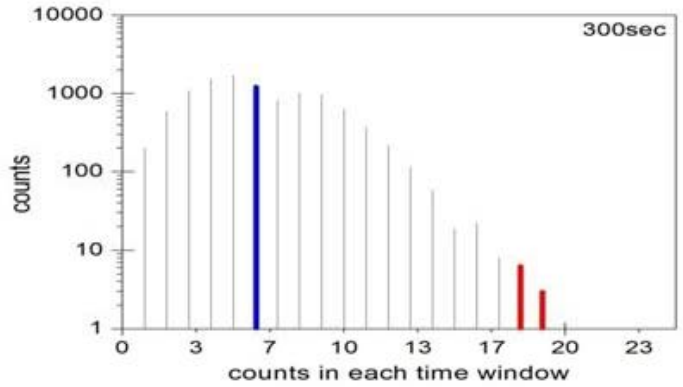

17/115=0.147

235/7909=0.029

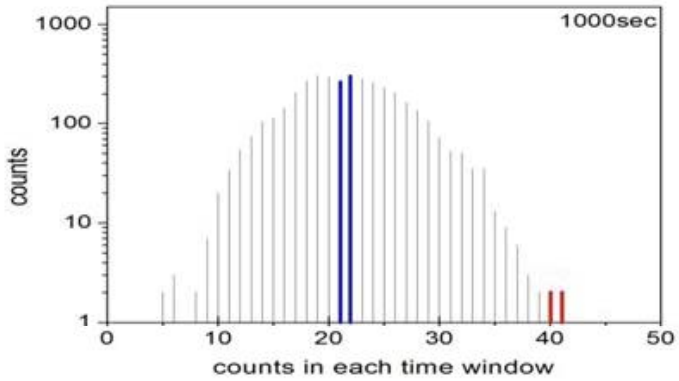

17/142=0.119

235/10808=0.021

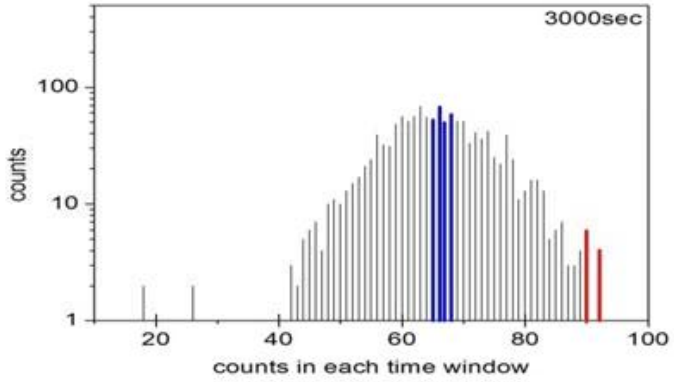

17/791=0.021

235/13034=0.018

In this figure counts in adjacent windows in three time window scales (300sec,1000sec and 3000sec) are presented and in any scale a window is signed which contains 17 probable gamma ray events .

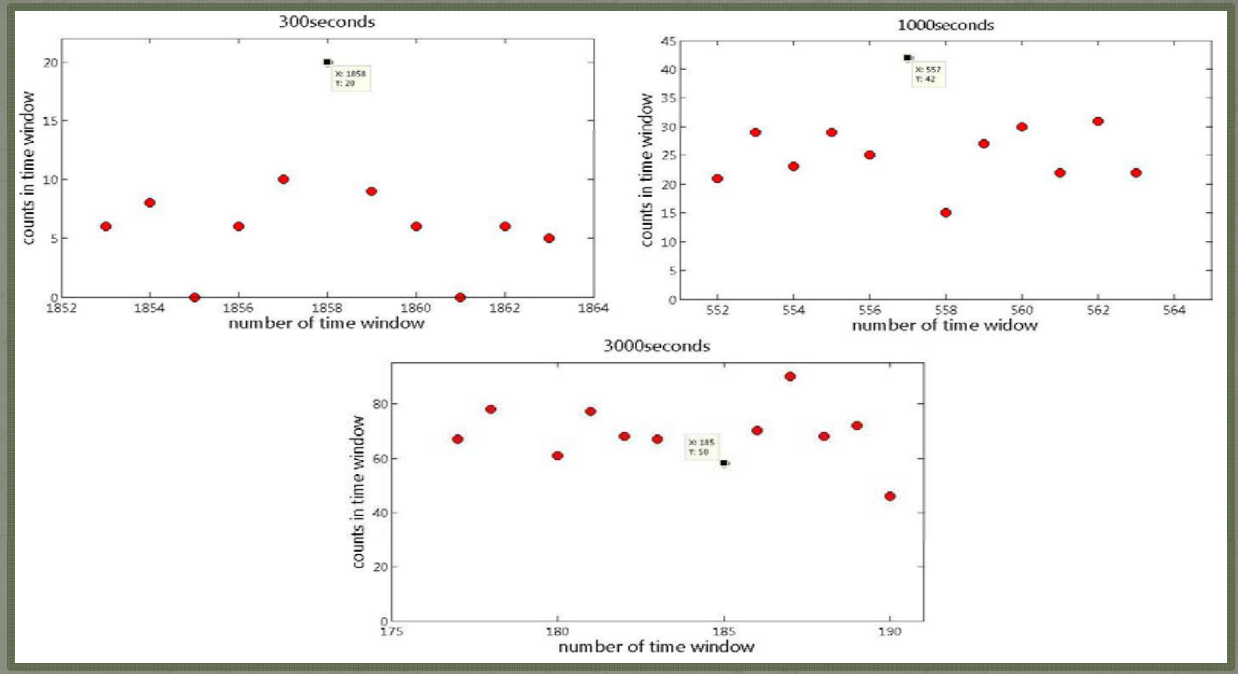

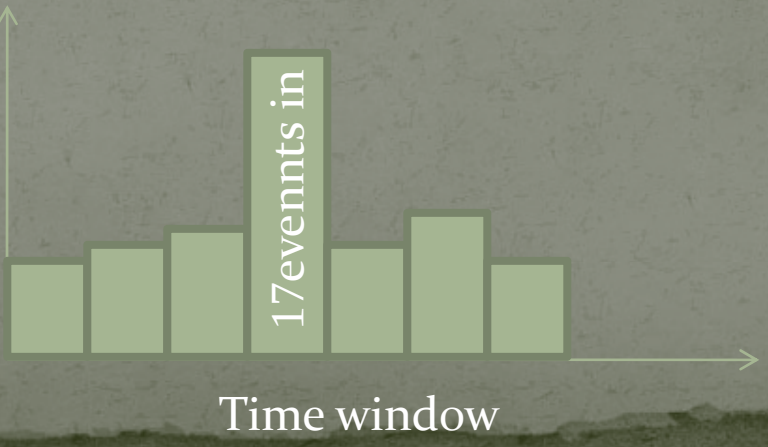

Location of 17 events with EGRET sources near to them . Areas around each source are angular resolution of the WCD array.

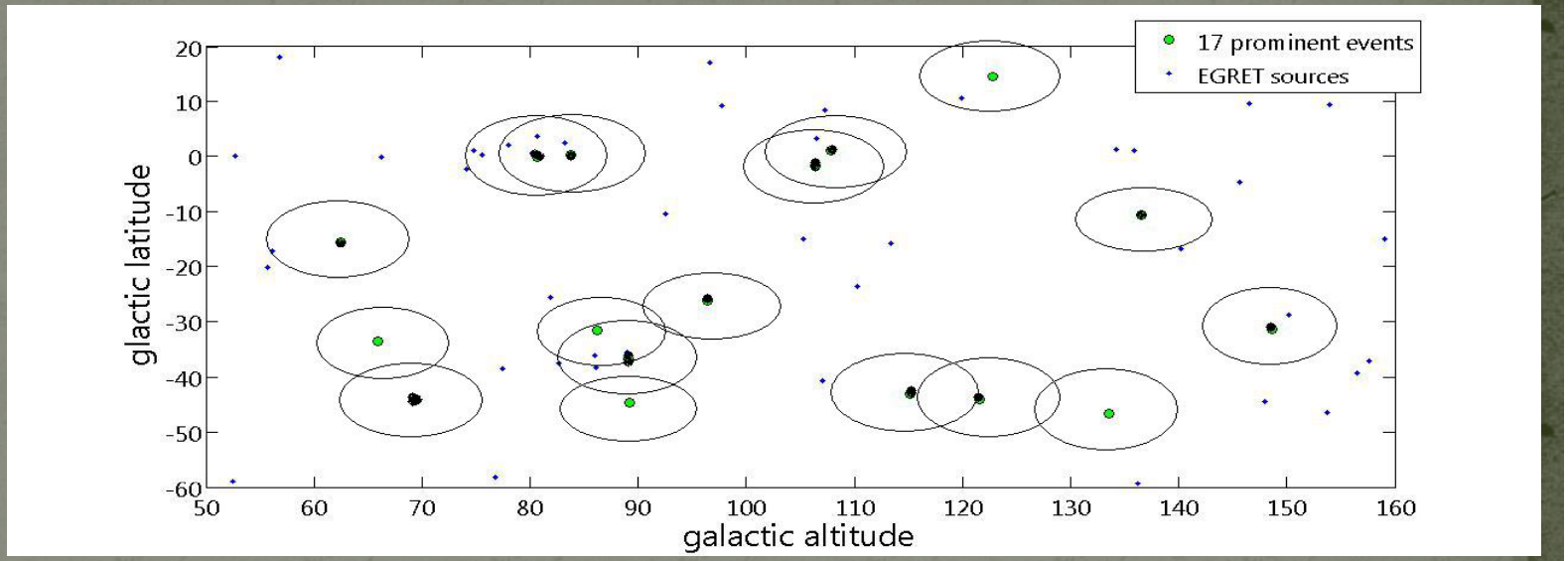

Most probable EGRET sources related to found events	Galactic coordinate of events l	b
3EG J2036+1131	62.4	-15.7
3EG J2016+3655, 3EG J2021+3716, 3EG J2021+4018, 3EG J2021+4316, 3EG 2033+4119	80.6	-0.06
3EG J2021+4018, 3EG J2021+4316, 3EG J2033+4119	83.7	0.1
3EG J2248+1746, 3EG J2254+1601	89.1	-44.6
3EG J2248+1746	86.1	-31.5
3EG J2227+6122	107.8	1.0
3EG J2227+6122	106	-1.8
3EG J0010+3710	122.7	14.4
3EG J0240+2816	148.6	-31.3

- By employing Li-Ma method, we observed some prominent sources probably related to some EGRET sources, but with this small amount of data and poor angular resolution we can't firmly claim that these prominences are referred to any EGRET source. Therefore for the next steps we are going to growth our detector resolusion and also resolusion of our array by increasing dimension of the array.

- We applied another method to observe any EAS event pointing to a gamma ray source. Among our data 17 of the EAS events were more probable to belong to a gamma ray source.

In order to have more precise array, two simulations were performed to find an optimum size for Cherenkov detectors, will be used in the next array. In the first simulation height of 60cm and diameter of 40cm is an optimum size for the water detector. The next simulation and experiments data approved this size to be the optimum size.


Thanks for your attention